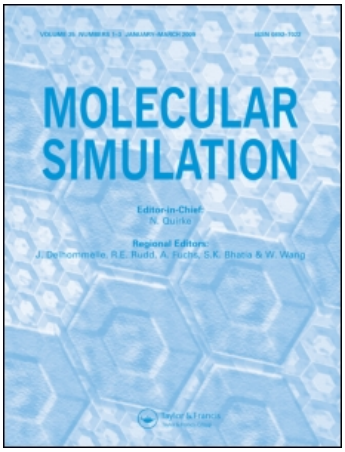

Molecular Simulation
Publication details, including instructions for authors and subscription information:
http://www.informaworld.com/smpp/title~content=t713644482

Atomistic Simulations of Uniaxial Tensile Behaviors of Single-walled Carbon Nanotubes

P. Liu[a]; Y. W. Zhang[b]; H. P. Lee[a]; C. Lu[a]
[a] Institute of High Performance Computing, Singapore [b] Department of Materials Science, Block SIA, National University of Singapore, Singapore, Singapore

To cite this Article Liu, P. , Zhang, Y. W. , Lee, H. P. and Lu, C.(2004) 'Atomistic Simulations of Uniaxial Tensile Behaviors of Single-walled Carbon Nanotubes', Molecular Simulation, 30: 8, 543 — 547
To link to this Article: DOI: 10.1080/08927020410001704951
URL: http://dx.doi.org/10.1080/08927020410001704951

Molecular Simulation, Vol. 30 (8), 15 July 2004, pp. 543–547

Taylor & Francis
Taylor & Francis Group

Atomistic Simulations of Uniaxial Tensile Behaviors of Single-walled Carbon Nanotubes

P. LIU[a], Y.W. ZHANG[b,*], H.P. LEE[a] and C. LU[a]

[a]*Institute of High Performance Computing, Singapore;* [b]*Department of Materials Science, Block SIA 02-10, National University of Singapore, 10 Science Drive, 4 Lower Kent Ridge Road, Singapore, Singapore 117543*

(Received March 2004; In final form April 2004)

Atomistic simulations, using the second-generation reactive empirical bond order (REBO) potential, are performed to investigate the uniaxial tensile behaviors of single-walled carbon nanotubes (SWCNTs). It is found that the effect of the nanotube diameters on the elastic modulus, the tensile strength and the stress vs. strain relation of SWCNTs is small yet noticeable. However, the effect of the degree of helicity is significant.

Keywords: Nanotube; Atomistic simulation; Carbon nanotube; Mechanical properties

INTRODUCTION

Carbon nanotubes exhibiting high stiffness, tensile strength and resilience have attracted much research interest. Direct measurements of mechanical properties are difficult to perform on nanotubes—however, many researchers manage to obtain their elastic modulus [1–4], tensile strength [4–6], defect structures and failure behaviors [3,7,8]. Meanwhile, atomistic simulations have been used to study the mechanical behaviors of nanotubes [9–24]. Due to the small size and the use of different experimental and simulation techniques, many conflicting results have been reported. For example, some researchers showed that nanotubes are extremely resilient [7,9,10,15,23], while others showed that they could be relatively brittle [4,5,21,22]. Some researchers have reported that the mechanical properties of nanotubes are insensitive to diameters and the degree of helicity [9–11,24], while others reported a wide range of dispersion: the reported axial elastic modulus values range from 0.2 to 5.5 TPa [3,4,19] and the reported tensile strength values vary from 0.005 to 0.093 TPa [3–6,19,23]. So far there is no consensus or unified understanding on the mechanical behaviors of nanotubes.

The measurements of mechanical properties of single-walled carbon nanotubes (SWCNTs) are even more challenging due to their small size and the tendency for bundle formation. It is believed that their elastic modulus and tensile strength should be higher than their multi-walled counterparts [3]. To date, atomistic simulations still cannot provide the conclusive proof of this due to the wide range of predicted dispersions. So far, most of the simulations make use of the first-generation of reactive empirical bond order (REBO) potential [25]. Recently, the second-generation of REBO potential [26] has been proposed: this contains improved analytical functions and an extended database as compared to the earlier version. This leads to a much better description of chemical and mechanical properties for hydrocarbon molecules and diamond [14,26,27]. Since the cutoff distance of the second-generation of REBO has been extended to 2 Å, which is beyond the inflection point 1.85 Å, it is able to describe bond breaking and rehybridization [27]. Hence, it is anticipated that the second generation REBO potential will be able to provide a better description for the mechanical properties of carbon nanotubes.

MODEL

In the present work, systematic atomistic simulations using the second-generation REBO potential [26] have been performed to study the effects of

*Corresponding author. E-mail: maszyw@nus.edu.sg

ISSN 0892-7022 print/ISSN 1029-0435 online © 2004 Taylor & Francis Ltd
DOI: 10.1080/08927020410001704951

the diameter and the degree of helicity on the axial tensile deformation behaviors of SWCNTs. The simulation temperature is 0K. The leapfrog method is used in numerical integration. For a SWCNT, the end atoms are displaced along the axial direction by small time steps. Subsequently the whole tube is relaxed by a velocity damping method to allow the atoms to reach mechanical equilibrium state while the two ends are fixed. Once the equilibrium state is reached, the stress of each atom in the SWCNT is calculated using

$$\sigma_{ij}^{m} = \frac{1}{\Omega_0}\frac{\partial U_m}{\partial \varepsilon_{ij}^{m}},$$

where σ_{ij}^{m}, U_m and ε_{ij}^{m} are the first Piola–Kirchhoff stress, the potential energy and the Lagrange strain of atom m, respectively; Ω_0 is the atomic volume at the reference state.

Different atomic volumes for the reference state have been used [10,12,20]. Since the stress is dependent on the choice of Ω_0, the value of Ω_0 will affect the stress and elastic modulus levels. The surface area occupied by a single carbon atom in the reference state is

$$S_0 = \frac{3\sqrt{3}a_0^2}{4},$$

where a_0 is the C—C bond length in the reference state. Here, the atomic volume in the reference state is taken as

$$\Omega_0 = \frac{3\sqrt{3}a_0^2 b_0}{4},$$

where $b_0 = 0.34\,\text{nm}$, which is the wall–wall separation. The Lagrange strain is calculated as

$$\varepsilon_{ij}^{m} = \frac{\left(F_{ik}^{m} F_{kj}^{m} - \delta_{ij}\right)}{2},$$

where F_{ij}^{m} is the deformation gradient of atom m and δ_{ij} is the Kronecker symbol. Since the deformation gradient is a two point tensor, F_{ij}^{m} is calculated by averaging over its neighboring atoms:

$$F_{ij}^{m} = \sum_{n=1}^{N}\left(\frac{r_i^{mn}}{R_j^{mn}}\right),$$

where r_i^{mn} and R_j^{mn} are the i- and j-th distance components between atoms m and n in the deformed and the reference configurations, respectively; N is the total number of the neighboring atoms within the cut-off distance of atom m. Hence the deformation gradient, strain and stress of an individual atom in SWCNTs can be obtained.

RESULTS AND DISCUSSIONS

The parametric study shows that as long as the length of the unfixed segment of a SWCNT is three times larger than the tube diameter, the deformation gradient at the central part of the nanotube is uniform and not affected by the loading at the ends. The uniform deformation gives rise to a uniform stress and strain distribution. Three typical examples of the central parts of the reference and deformed configurations for three different degrees of helicity of SWCNTs: $\theta = 0°$, 20° and 30° are given in Fig. 1. (The degree of helicity is described by θ, where $0° \le \theta \le 30°$. $\theta = 0°$ for zigzag configurations and $\theta = 30°$ for armchair configurations [9].) For the deformed configurations, the uniaxial strain level is 0.15. (The strain level is at the central part of the nanotubes.) The diameters of the SWCNTs are 1.8 nm. It can be clearly seen that upon the axial tension, the deformation at the central parts of the nanotubes is very uniform. However, the hexagonal atomic arrangements in the reference states have

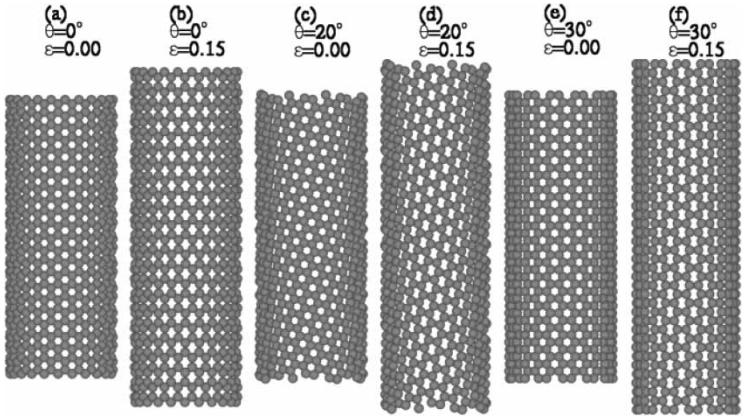

FIGURE 1 (a) and (b) are the reference and deformed SWCNTs for $\theta = 0°$, (c) and (d) for $\theta = 20°$, and (e) and (f) for $\theta = 30°$, respectively. The initial diameters are 1.8 nm. The uniaxial strains for the deformed SWCNTs are 0.15. (Only the central parts of the nanotubes with uniform deformation are shown).

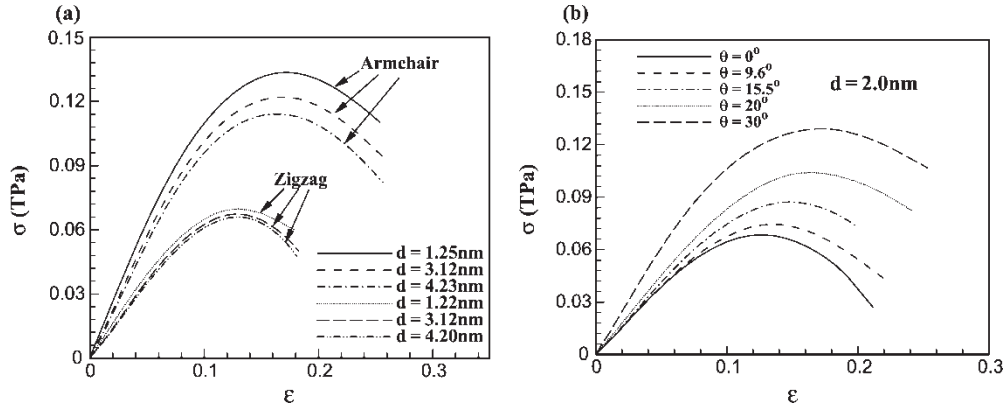

FIGURE 2 Variations of stress vs. strain with the changes in the diameter and with the degree of helicity of SWCNTs. (a) Change in the diameter for armchair and zigzag SWCNTs. (b) Change in the degree of helicity at a diameter of $d = 2.0$ nm.

been severely distorted and elongated along the axial direction upon loading. The present atomistic simulations allow one to fully explore the effects of the diameters and the degrees of helicity of SWCNTs on the tensile behaviors.

The stress vs. strain curves for the armchair and zigzag configurations at different diameters and for different degrees of helicity at a fixed diameter are shown in Fig. 2(a) and (b), respectively. Two important features can be clearly seen from the graphs. (1) The effect of the degree of helicity on the stress vs. strain relations is significant. The elastic moduli, the tensile strengths and the whole stress vs. strain curves of the armchair nanotubes are much higher in value than those of the zigzag nanotubes. (The elastic modulus is calculated by the slope of the axial stress vs. the axial strain curves at the point of zero strain). (2) The effect of the nanotube diameters on the elastic modulus, the tensile strength and the stress vs. strain relations is small yet noticeable.

The variations of the elastic modulus of SWCNTs with diameter at three different degrees of helicity and with the degree of helicity at three different diameters are shown in Fig. 3(a) and (b), respectively. The change in elastic modulus with diameter follows a similar tendency for different values of helicity θ. When the nanotube diameter is small, the elastic modulus increases with an increase in diameter. This change can be explained by large curvatures of small nanotubes, which distort the C—C bonds, therefore reducing the elastic modulus. However, when the diameter is large, the elastic modulus decreases with an increase in diameter. The maximum elastic modulus for an armchair SWCNT occurs at approximately 1.0 nm, while for the zigzag SWCNT, it is approximately at 1.3 nm. The reason for this decrease is not yet clear. For large diameters, all curves level off and approach constants with an average value of 0.97 TPa. As the degree of helicity increases, so too does the elastic modulus. When the degree of helicity is low, the increment is slow. It appears that there is a transitional degree of helicity after which the increment in the elastic modulus is severe. For example, the transitional degree of helicity is approximately 27° for $d = 4.20$ nm, while 20° for $d = 0.95$ nm. The variation

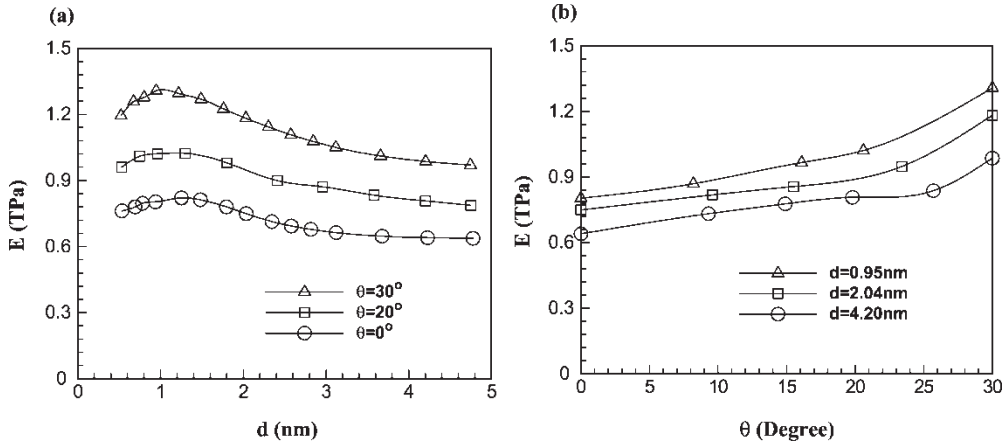

FIGURE 3 Variations of elastic modulus with changes in the diameter and with the degree of helicity of SWCNTs. (a) Change in the diameter at three different degrees of helicity. (b) Change in the degree of helicity at three different diameters.

of elastic modulus with the degree of helicity can be explained by the nature of interatomic bond strength and bond orientations. In zigzag nanotubes, one-third of the bonds are aligned along the axial direction. During axial tension, all of the bonds are stretched, that is they are under tension. The resistance to the lateral deformation of SWCNTs is mainly associated with the change in bond angles (see Fig. 1(b)). However, for armchair nanotubes, one-third of the bonds are perpendicular to the loading directions. During axial tension, these bonds are in compression, providing a stronger resistance to the lateral deformation than that of zigzag nanotubes (see Fig. 1(f)). As a consequence, the elastic modulus of armchair nanotubes is higher than that of zigzag nanotubes. When the degree of helicity slightly shifts away from the armchair configuration, the compression of these bonds quickly turns into tension. This explains the severe decrease in elastic modulus when the degree of helicity slightly deviates from the armchair configurations.

The variations of tensile strength with diameter at three different degrees of helicity and with the degree of helicity at three different diameters are shown in Fig. 4(a) and (b), respectively. It is shown that there is an approximately linear relationship between the diameter and the tensile strength. As the diameter increases, the tensile strength of the nanotubes decreases. The absolute values of the slopes increase with an increase in the degree of helicity. For the zigzag nanotubes, the curve is almost flat, indicating that the tensile strength is insensitive to the diameter of the nanotubes. The variations of tensile strength with the degree of helicity at different diameters show a similar tendency and exhibit a sigmoidal shape. There are three stages in the curves. Stages I and III are relatively flat, compared with the slope of Stage II. It is believed that the tensile strength is related to the elastic modulus of nanotubes [28], therefore the reason for the influence of diameter and the degree of helicity on the elastic modulus may also be used to explain the change in the tensile strength.

In the present simulations, the elastic modulus varies from 0.68 to 1.30 TPa and the tensile strength varies from 0.066 to 0.131 TPa with a variation of the diameter and the degree of helicity. The previously measured and predicted values of elastic modulus for carbon nanotubes range from 0.2 to 5.5 TPa. Therefore the range of the present predicted elastic modulus lies in the middle of the previous results. The average value of the present simulation results is 0.97 TPa, which is close to the in-plane elastic modulus of graphite, 1.06 TPa. The reported tensile strength varies from 0.005 to 0.093 TPa [3–6,19,23]. It is believed that these previously reported values may be too low [6]. The predicted range here is higher than the previously predicted one. The tensile strength has been related to the elastic modulus [28] by $\sigma_b = \beta Y$, where σ_b and Y are the tensile strength and the elastic modulus for perfect nanotubes, respectively; and β is the proportionality constant, which ranges from 0.05 to 0.1 [28]. Since the present predicted range for elastic modulus is from 0.68 to 1.30 TPa, the above relation predicts that the tensile strength for perfect nanotubes ranges from 0.034 to 0.13 TPa, which lies in the upper part of the present prediction. It is observed that when the axial strain is larger than 0.05, the nonlinear elastic deformation becomes increasingly pronounced. Therefore, to fully utilize the mechanical properties of SWCNTs for accurate nanostructure designs, the data on elastic modulus and tensile strength are not enough, and an accurate stress and strain relation is necessary. The present simulations provide useful information for this purpose.

The elastic moduli obtained in the present paper are in agreement with the previous results [12,15,23,24], and the tensile strengths are slightly higher than that obtained by Yu [4] and Belytschko [23]. Interestingly, however, the present results

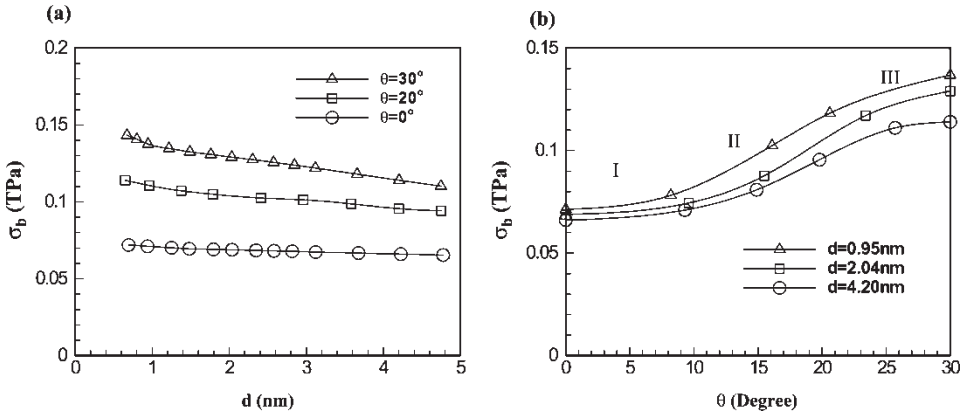

FIGURE 4 Variations of tensile strength with the changes in the diameter and with the degree of helicity of SWCNTs. (a) Change in the diameter at three different degrees of helicity. (b) Change in the degree of helicity at three different diameters.

predict that the effect of the diameter of the SWCNTs is small yet noticeable, and the effect of the degree of helicity is significant. These features are different from that obtained using the first-generation REBO potential and through the use of quantum mechanical methods, which have shown that the mechanical properties are either moderate or insensitive to the diameter and the degree of helicity of carbon nanotubes [10,11,23,24].

CONCLUSIONS

In conclusion, the second-generation REBO potential has been used to systematically study the effect of the diameter and the degree of helicity of SWCNTs on the axial tensile deformation behaviors. It is shown that the effect of the diameter of SWCNTs on the elastic modulus, the tensile strength and the stress vs. strain relation is small yet noticeable. However, the effect of the degree of helicity is significant. The present results may be used to explain the wide range of measured and predicted elastic moduli and tensile strengths and may provide useful information for the deformation behaviors of carbon nanotubes.

References

[1] Treacy, M.M.J., Ebbesen, T.W. and Gibson, J.M. (1996) "Exceptionally high Young's modulus observed for individual carbon nanotubes", *Nature* **381**, 678.

[2] Wong, E.W., Sheehan, P.E. and Lieber, C.M. (1997) "Nanobeam mechanics: elasticity, strength, and toughness of nanorods and nanotubes", *Science* **277**, 1971.

[3] Salvetat, J.P., Bonard, J.M., Thomson, N.H., Kulik, A.J., Forro, L., Benoit, W. and Zuppiroli, L. (1999) "Mechanical properties of carbon nanotubes", *Appl. Phys. A* **69**, 255.

[4] Yu, M.F., Files, B.S., Arepalli, S. and Ruoff, R.S. (2000) "Tensile loading of ropes of single wall carbon nanotubes and their mechanical properties", *Phys. Rev. Lett.* **84**, 5552.

[5] Walters, D.A., Ricson, L.M., Casavant, M.J., Liu, J., Colbert, D.T., Smith, K.A. and Smalley, R.E. (1999) "Elastic strain of freely suspended single-wall carbon nanotube ropes", *Appl. Phys. Lett.* **74**, 3803.

[6] Li, F., Cheng, H.M., Bai, S., Su, G. and Dresselhaus, M.S. (2000) "Tensile strength of single-walled carbon nanotubes directly measured from their macroscopic ropes", *Appl. Phys. Lett.* **77**, 3161.

[7] Falvo, M.R., Clary, G.J., Taylor, R.M., Chi, V., Brooks, F.P., Jr., Washburn, S. and Superfine, R. (1997) "Bending and buckling of carbon nanotubes under large strain", *Nature* **389**, 582.

[8] Chopra, N.G., Benedict, L.X., Crespi, V.H., Cohen, M.L., Louie, S.G. and Zettle, A. (1995) "Fully collapsed carbon nanotubes", *Nature* **377**, 135.

[9] Yakobson, B.I. and Avouris, P. (2001) "Mechanical properties of carbon nanotubes", *Top. Appl. Phys.* **80**, 287.

[10] Yakobson, B.I., Brabec, C.J. and Bernholc, J. (1996) "Nanomechanics of carbon tubes: instabilities beyond linear response", *Phys. Rev. Lett.* **76**, 2511.

[11] Hernandez, E., Goze, C., Bernier, P. and Rubio, A. (1999) "Elastic properties of single-wall nanotubes", *Appl. Phys. A* **68**, 287.

[12] Lu, J.P. (1997) "Elastic properties of carbon nanotubes and nanoropes", *Phys. Rev. Lett.* **79**, 1297.

[13] Krishnan, A., Dujardin, E., Ebbesen, T.W., Yianilos, P.N. and Treacy, M.M.J. (1998) "Young's modulus of single-walled nanotubes", *Phys. Rev. B* **58**, 14013.

[14] Sinnott, S.B., Shenderova, O.A., White, C.T. and Brenner, D.W. (1998) "Mechanical properties of nanotubule fibers and composites determined from theoretical calculations and simulations", *Carbon* **36**, 1.

[15] Salvetat, J.P., Briggs, G.A., Bonard, J.M., Bacsa, R.R., Kulik, A.J., Stockli, T., Burnham, N.A. and Forro, L. (1999) "Elastic and shear moduli of single-walled carbon nanotube ropes", *Phys. Rev. Lett.* **82**, 944.

[16] Srivastava, D., Menon, M. and Cho, K. (1999) "Nanoplasticity of single-wall carbon nanotubes under uniaxial compression", *Phys. Rev. Lett.* **83**, 2973.

[17] Wei, C.Y., Cho, K.J. and Srivastava, D. (2003) "Tensile strength of carbon nanotubes under realistic temperature and strain rate", *Phys. Rev. B* **67**, 115407.

[18] Popov, V.N., Van Doren, V.E. and Balkanski, M. (2000) "Elastic properties of single-walled carbon nanotubes", *Phys. Rev. B* **61**, 3078.

[19] Dereli, G. and Ozdogan, C. (2003) "Structural stability and energetics of single-walled carbon nanotubes under uniaxial strain", *Phys. Rev. B* **67**, 035416.

[20] Kudin, K.N., Scuseria, G.E. and Yakobson, B.I. (2001) "C_2F, BN, and C nanoshell elasticity from *ab initio* computations", *Phys. Rev. B* **64**, 235406.

[21] Zhao, Q., Nardelli, M.B. and Bernholc, J. (2002) "Ultimate strength of carbon nanotubes: a theoretical study", *Phys. Rev. B* **65**, 144105.

[22] Nardelli, M.B., Fattebert, J.L., Orlikowski, D., Roland, C., Zhao, Q. and Bernholc, J. (2000) "Mechanical properties, defects and electronic behavior of carbon nanotubes", *Carbon* **38**, 1703.

[23] Belytschko, T., Xiao, S.P., Schatz, G.C. and Ruoff, R. (2002) "Atomistic simulations of nanotube fracture", *Phys. Rev. B* **65**, 235430.

[24] Sanchez-Portal, D., Artacho, E., Soler, J.M., Rubio, A. and Ordejon, P. (1999) "*Ab initio* structural, elastic, and vibrational properties of carbon nanotubes", *Phys. Rev. B* **59**, 12678.

[25] Brenner, D.W. (1990) "Empirical potential for hydrocarbons for use in simulating the chemical vapor deposition of diamond films", *Phys. Rev. B* **42**, 9458.

[26] Brenner, D.W., Shenderova, O.A., Harrison, J.A., Stuart, S.J., Ni, B. and Sinnott, S.B. (2002) "A second-generation reactive empirical bond order (REBO) potential energy expression for hydrocarbons", *J. Phys. Condens. Matter* **14**, 783.

[27] Shenderova, O.A., Brenner, D.W., Omeltchenko, A., Su, X. and Yang, L.H. (2000) "Atomistic modeling of the fracture of polycrystalline diamond", *Phys. Rev. B* **61**, 3877.

[28] Ruoff, R.S. and Lorents, D.C. (1995) "Mechanical and thermal properties of carbon nanotubes", *Carbon* **33**, 925.